

# Application-Driven Objectives

Advance Your Research



# Objectives that Enable Innovative Research

With a rich history in optical design, Evident develops high-quality objectives for advanced life science applications. We work with our customers to develop innovative products that meet both the evolving and specific needs of researchers in the field.

Our commitment to innovative optical technologies is exemplified by our multiphoton excitation dedicated objectives, which we developed in response to the growing need for deep tissue observation in life science research. When our customers needed an optical system designed for live cell and *in vivo* 3D imaging, we developed silicone immersion objectives that enable researchers to capture bright, high-resolution images deeper within samples.

For more than 100 years, we have manufactured advanced microscope equipment and high-quality objectives, and we are proud of our record of innovation and collaboration. We continue to work with researchers to develop new technologies that meet the changing needs of life science research.



## *Index*

---

Considerations for Choosing an Objective and Using a Correction Collar .....	2
Multiphoton Excitation (MPE) Dedicated Objectives .....	3-4
Silicone Immersion Objectives .....	5-6
High-Resolution Objectives for Super Resolution and TIRF .....	7-8
Super-Corrected Objective .....	9
Save Time Imaging Plastic-Bottom Plates and Dishes .....	10

## Choosing an Objective for Your Research Application

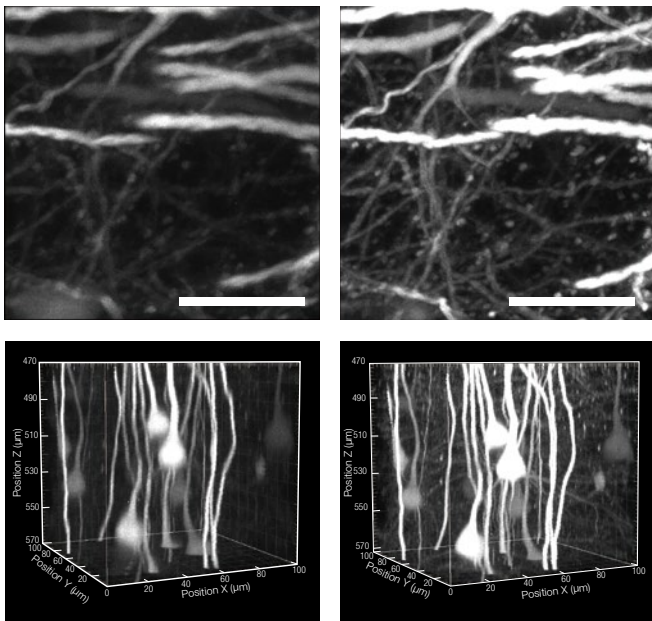
Selecting the right objective for your research application is essential to obtain high-resolution images. By matching the refractive index of the sample and immersion medium, the objective can compensate for spherical aberration and produce deeper, brighter, and higher resolution images. Most of our A Line™ objectives have high numerical apertures (NAs) and correction collars that enable users to compensate for spherical aberration, enhancing image resolution and contrast.

## The Importance of a Correction Collar

Spherical aberration is influenced by refractive index mismatches in the optical path, such as variable coverslip thickness, a sample's observation depth, the composition of cells or tissues, and changes in temperature. High NA objectives are particularly susceptible to these effects. Adjusting your objective's correction collar is essential to compensate for spherical aberration and improve image quality. The result is higher resolution, brighter, and higher contrast images.

If you are using an inverted microscope, the remote collar control unit (IX3-RCC) greatly improves the usability of correction collars. For deep imaging with an upright multiphoton laser scanning microscope, TruResolution™ objectives (FV30-AC10SV and FV30-AC25W) offer a powerful auto-adjust correction collar.

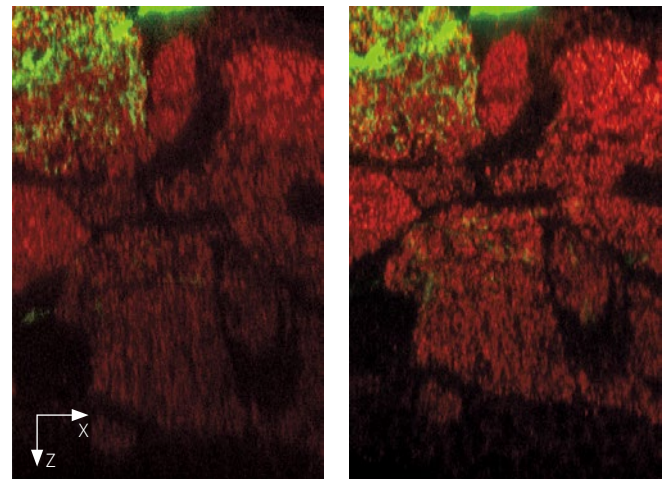
### An image of an *in vivo* mouse brain sensory cortex before (left) and after (right) adjusting the XLPLN25XWMP2 objective's correction collar.



Upper figures: XZ image at 500  $\mu\text{m}$  depth; scale bar represents 20  $\mu\text{m}$ .  
Lower figures: XYZ image at 470–570  $\mu\text{m}$  depth.

Sample: Th1-YFP-H mouse

### Comparison of oil and silicone immersion 60X objectives in a glycerol-mounted *Drosophila* brain.



Oil immersion

Silicone immersion

mCD8 (GFP, Green)/ $\alpha$ -Bruchpilot (Immunostaining, Red)

Image data courtesy of:  
Yasuhiro Imanishi Ph.D., Hiromu Tanimoto Ph.D.  
Tohoku University Graduate School of Life Sciences



IX3-RCC remote collar control unit



FV30-AC25W (25X water dipping objective; NA: 1.05; W.D.: 2 mm)

# Multiphoton Excitation Dedicated Objectives

Designed to achieve optimum performance during multiphoton excitation (MPE) imaging of *in vivo* and transparent samples, these objectives enable high-precision imaging to a depth of 8 mm.



## MPE Dedicated Objectives

	W.D. (mm)	MAG.	OFN*	NA	Immersion (Refractive Index)	Sample	Purpose
XLPLN10XSVM	8	10X	18	0.60	Water to oil (ne: 1.33 to 1.52)	<i>in vivo</i> and cleared sample	Wide FOV observation
XLPLN25XGMP	8	25X	18	1.00	Silicone oil to oil (ne: 1.41 to 1.52)	Cleared sample	High-resolution observation
XLPLN25XSVM	8	25X	18	0.95	Water to silicone oil (ne: 1.33 to 1.41)	<i>in vivo</i> and cleared sample	
XLPLN25XSVM2	4	25X	18	1.00	Water to silicone oil (ne: 1.33 to 1.41)	<i>in vivo</i> and cleared sample	
XLPLN25XWMP2	2	25X	18	1.05	Water (ne: 1.33)	<i>in vivo</i>	
FV30-AC10SV	8	10X	18	0.60	Water to oil (ne: 1.33 to 1.52)	<i>in vivo</i> and cleared sample	Wide FOV observation
FV30-AC25W	2	25X	18	1.05	Water (ne: 1.33)	<i>in vivo</i>	High-resolution observation

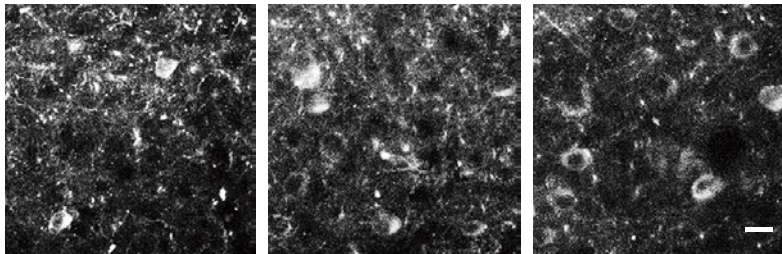
\*Maximum field number observable through eyepiece.

## Deep In Vivo Imaging with the XLPLN25XWMP2 Objective

Deep *in vivo*, multiphoton brain imaging, and optogenetics at high-resolution require objectives with high infrared (IR) light transmission, a high numerical aperture (NA), and the ability to correct for the depth and scattering of tissue. The XLPLN25XWMP2 objective delivers broad IR transmission with the new 1600 coating, enabling optogenetic stimulation with visible light down to 400 nm and IR imaging or stimulation beyond 1600 nm. The correction collar reduces the excitation volume, enabling stimulation of single cells or dendritic spines. Combined with the powerful and precise scanning capabilities of the FV4000MPE multiphoton laser scanning microscope, the XLPLN25XWMP2 objective is the right tool for high-precision multiphoton imaging.

### In Vivo Two-Photon Imaging of Crossed Corticostriatal and Corticospinal Neurons in L5a During Learning

- Calcium imaging of a deep brain neuron circuit enables researchers to observe bright, quick responses of single neuron activity.

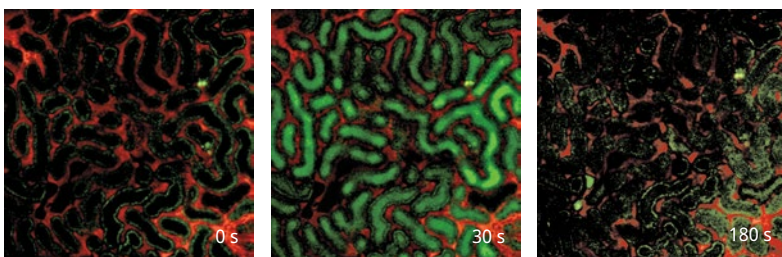


450 μm depth from brain surface    500 μm depth from brain surface    550 μm depth from brain surface

*in vivo* two-photon imaging of crossed corticostriatal neurons transduced with rAAV2/9-Syn-GCaMP3 in the left forelimb M1 during learning of a motor task. 450, 500, and 550 μm depth from brain surface. Scale bar 20 μm. Image data courtesy of Yoshito Masamizu Ph.D., Yasuhiro R Tanaka Ph.D., Masanori Matsuzaki Ph.D., Division of Brain Circuits, National Institute for Basic Biology. Reference: *Nat Neurosci.* 2014 Jul; 17 (7): 987-94. doi: 10.1038/nn.3739. Epub 2014 Jun 1.

### In Vivo Nephron Imaging at Kidney Surface

- High-resolution *in vivo* time-lapse imaging with a 1.05 NA.

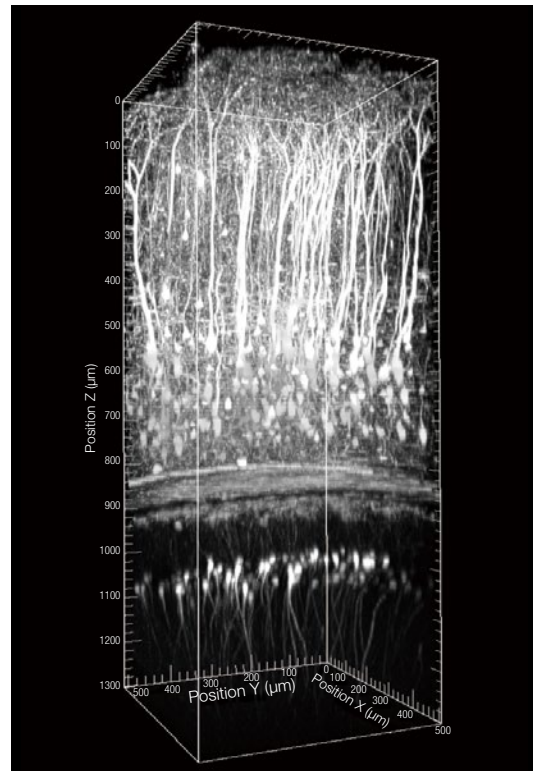


Time-lapse imaging of fluorescence dye (Lucifer Yellow, Green) injected into a vein that freely passes through the glomerulus. Red is rhodamine B labeled 70 kD dextran to observe the flow of blood plasma. The shadows in the blood plasma are blood cells. The green signal at 0 time is auto fluorescence of the proximal tubular cell.

Image data courtesy of Daisuke Nakano Ph.D., Department of Pharmacology, Faculty of Medicine, Kagawa University. Reference: *J Am Soc Nephrol.* 2015 Apr 8. pii: ASN.2014060577. [Epub ahead of print]

### Deep Mouse Brain Imaging

- Image deep within a mouse brain thanks to high NA objectives with a 2 mm working distance and optimized correction collar adjustments.



Z-stack image of *in vivo* mouse under anesthesia from the brain surface to the radiate layer of the hippocampus (CA1).

Sample: Thy1-YFP H line 8-week-old male  
Excitation wavelength: 960 nm  
Image data courtesy of Katsuya Ozawa and Hajime Hirase, Neuron-Glia Circuitry, RIKEN Brain Science Institute, Japan

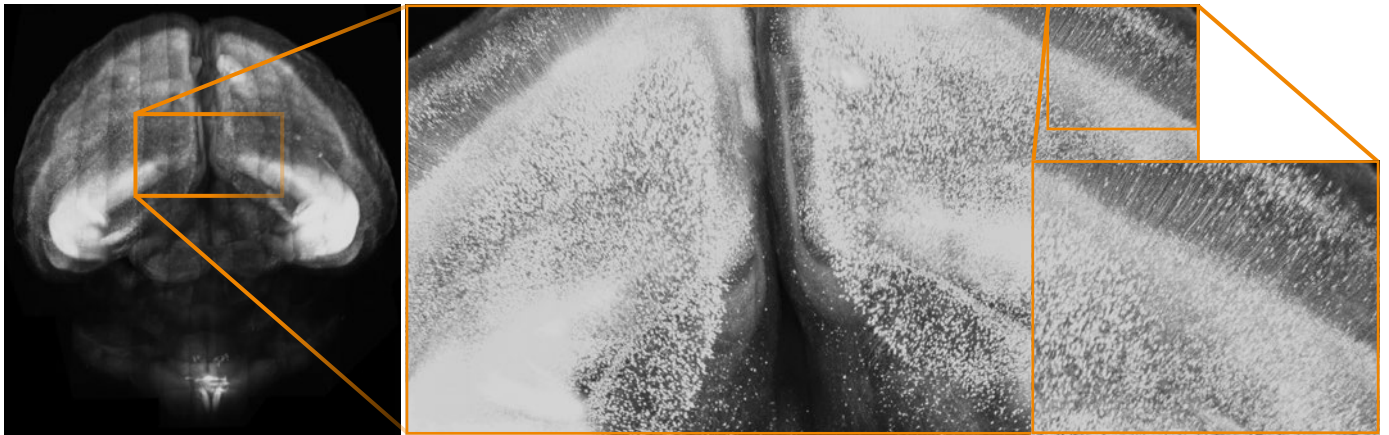
## Observing Fixed Transparent Specimens to a Depth of 8 mm Using Multiphoton Dedicated Objectives

Our MPE dedicated objectives help facilitate breakthrough research on brain function and other vital organs. Until recently, brain science researchers using light microscopes had to slice thin sections of tissue. Using MPE dedicated objectives and tissue clearing technology, researchers can see up to 8 mm deep without slicing. The XLPLN25XSVM2 and XLSLPLN25XSVM2 objectives were engineered for use with the revolutionary clearing reagent "Sca/e" developed by Dr. Atsushi Miyawaki and his team at the RIKEN Brain Science Institute in Japan.\* The XLSLPLN25XGMP and XLPLN10XSVM objectives support many reagents, including SeeDB, CLARITY, and Sca/eS, enabling researchers to observe down to unprecedented depths and see the interconnections in the brain and other tissues as never before.

\*Published online in *Nature Neuroscience*: Hama et al. Aug 30, 2011

### Whole Mouse Brain Imaging (XLPLN10XSVM)

- Wide field of view with 10X magnification, single-cell resolution with a 1.0 NA, and observations down to 8 mm.
- Objectives match a wide range of clearing reagent refractive indices (ne: 1.33 to 1.52).



20-week-old YFP-H mouse brain treated with Sca/eS

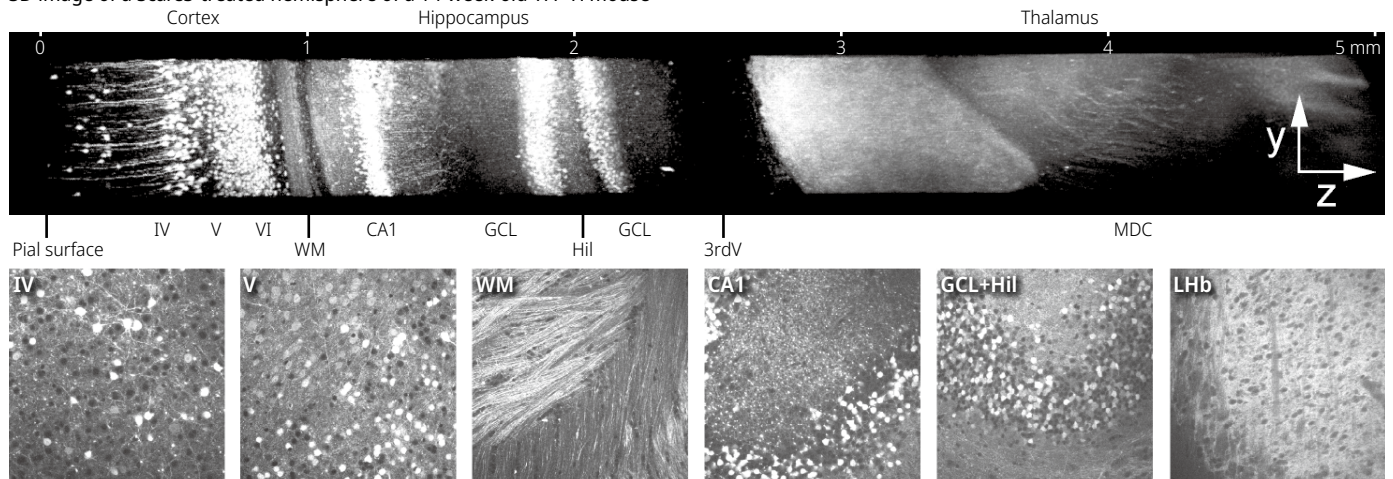
Image data courtesy of Hiroshi Hama, Atsushi Miyawaki, Laboratory for Cell Function Dynamics, RIKEN Center for Brain Science

Single-cell resolution

### High-Resolution Deep Brain Imaging of Sca/eS-Treated Mouse Brain (XLSLPLN25XGMP)

- High-resolution deep imaging with a 1.0 NA and an 8 mm W.D.
- Objectives match the refractive index of clearing reagents (ne: 1.41 to 1.52).

3D image of a Sca/eS-treated hemisphere of a 14-week-old YFP-H mouse



A maximum intensity projection image (top). Six XY images at different Z positions (bottom). WM: white matter; GCL: granule cell layer, Hil: hilus, LHb: lateral habenular nucleus, MDC: mediodorsal thalamic nucleus; scale bars represent 0.1 mm.

Image data courtesy of Hiroshi Hama, Atsushi Miyawaki, Laboratory for Cell Function Dynamics, RIKEN Center for Brain Science  
Reference: *Nat Neurosci*. 2015 Oct; 18 (10): 1518–29. doi: 10.1038/nn.4107. Epub 2015 Sep 14.

# Silicone Immersion Objectives

Silicone immersion objectives are optimized for live cell and live tissue imaging. By properly matching the refractive index, images are clearer and brighter, and time-lapse observations become more reliable and less complex because silicone oil does not dry at 37 °C (98.6 °F). Unlike glycerol/water mixtures, the refractive index of silicone oil remains constant, and the resolution is higher than comparable water objectives, helping ensure the accuracy of critical cell and tissue morphology studies. Because the refractive index of silicone immersion oil ( $n_e=1.40$ ) is close to that of the clearing reagent SCALEVIEW-A2 ( $n_e=1.38$ ), the silicone immersion objectives are also well suited for observing SCALEVIEW-A2-cleared samples.

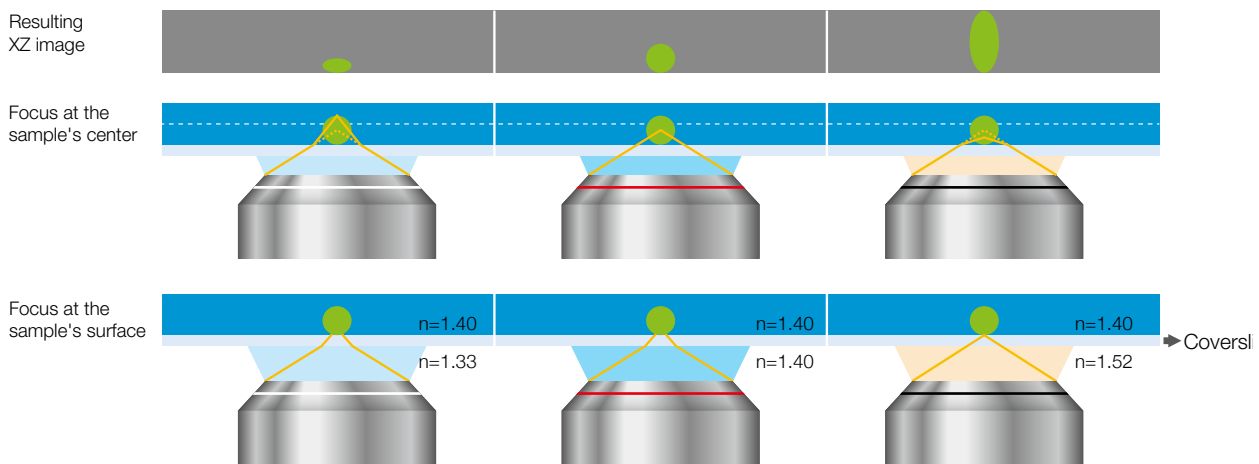


## Silicone Immersion Objectives

	W.D. (mm)	MAG.	OFN*	NA	Immersion	Applications
UPLSAPO100XS	0.2	100X	22	1.35	Silicone oil	High-resolution for subcellular imaging
UPLSAPO60XS2	0.3	60X	22	1.30	Silicone oil	High-resolution and long-term time-lapse imaging of single cells
UPLSAPO40XS	0.3	40X	22	1.25	Silicone oil	Multiple cell imaging with submicron resolution
UPLSAPO30XS	0.8	30X	22	1.05	Silicone oil	Deeper tissue imaging with a wider field of view
UPLSAPO30XSIR	0.8	30X	22	1.05	Silicone oil	MPE imaging in deep tissue with a wider field of view

\*Maximum field number observable through eyepiece.

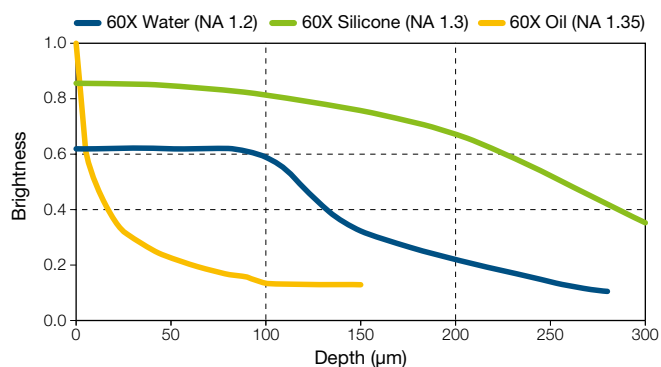
## Effects of Refractive Index Mismatch on Sample Shape



Matching the refractive index of a sample and immersion media is very important to get accurate 3D images.

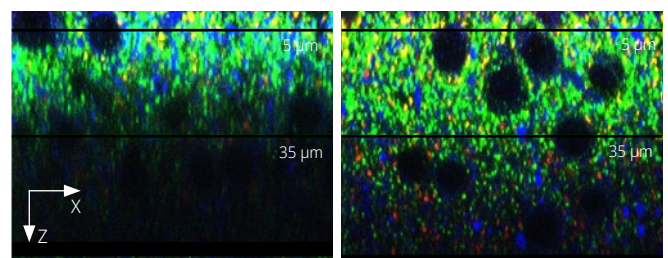
## Comparing the Brightness of 60X Objectives

Normalized by the brightness of the 60X objective at the sample's surface; sample refractive index: 1.38.



brighter than water immersion objectives at all focus depths for a given magnification.

## Comparison of Silicone and Oil Immersion 60X Objectives



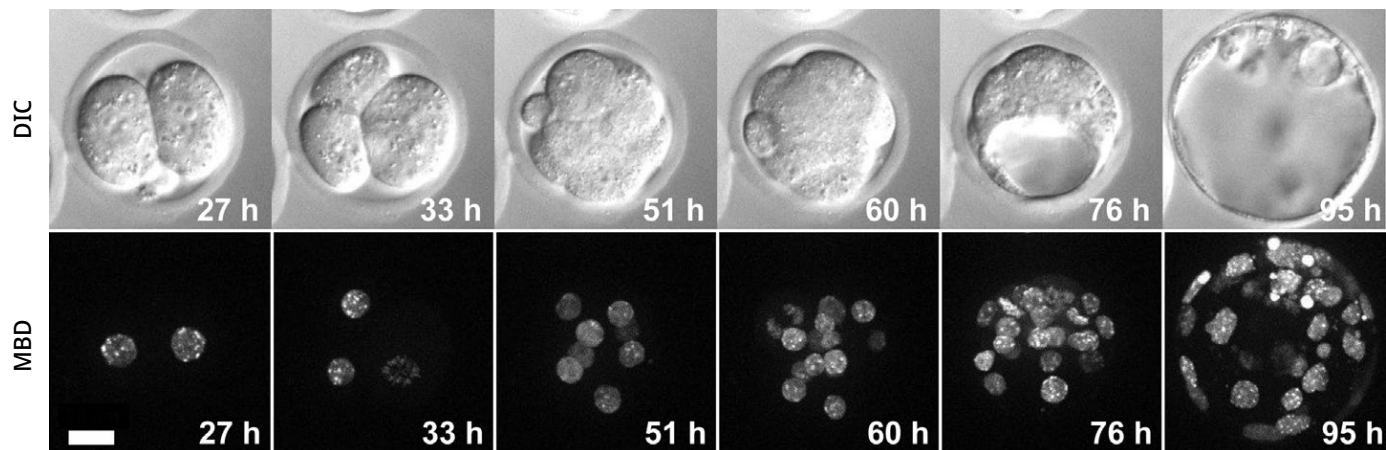
UPLSAPO 60XO (NA 1.3, W.D. 0.3 mm, immersion oil  $n_e = 1.52$ ) UPLSAPO60XS2 (NA 1.3, W.D. 0.3 mm, silicone oil  $n_e = 1.4$ )

By matching the refractive index of the sample and immersion medium, the silicone objective (UPLSAPO60XS2) enables deeper imaging.  
Sample: Sca/eA2-treated neocortex, VGluT1/Green, VGluT2/Red, MAP2/Blue

Image data courtesy of Motokazu Uchigashima, M.D., Ph.D., Masahiko Watanabe, M.D., Ph.D., Department of Anatomy, Hokkaido University Graduate School of Medicine

## Long-Term Time-Lapse Imaging of a Live Mouse Embryo (UPLSAPO60XS2)

- High-resolution imaging with 1.30 NA; 3D imaging with 0.3 mm W.D.
- Long-term time-lapse imaging with stable silicone immersion oil.



Long-term time-lapse images of a live mouse embryo. Images were taken every hour from the zygote (0 h) to blastocyst (119 h) stage. mCherry-fused methyl-CpG-binding domain (MBD) of MBD1 protein. Images acquired using silicone immersion objective UPLSAPO60XS. Scale bar, 20  $\mu\text{m}$ .

Image data courtesy of Kazuo Yamagata Ph.D., Faculty of Biology-Oriented Science and Technology, Kinki University  
Reference Stem: *Cell Reports*. 2014 Jun 3; 2 (6): 910–924.

## Three-Dimensional Observation of Biliary Tree Structures in Mouse Liver with a 30X Objective (UPLSAPO30XS)

To obtain higher resolution three-dimensional images, the FLUOVIEW™ confocal microscope and a 30X silicone oil immersion objective (UPLSAPO30XS: 1.05 NA, 0.8 mm WD) were used to obtain consecutive tomographic images (Z axial interval of 1  $\mu\text{m}$ ) of biliary tissue (green, biliary epithelial cell marker CK19) in 200  $\mu\text{m}$  thick liver tissue cleared using SeeDB. This combination enabled high-resolution observation of the biliary trees of control and Klf5-LKO mice while maintaining a wide field of view. In the Klf5-LKO mouse, researchers observed CK19+ cell clusters (white arrow) that were spatially separated from the biliary tree.

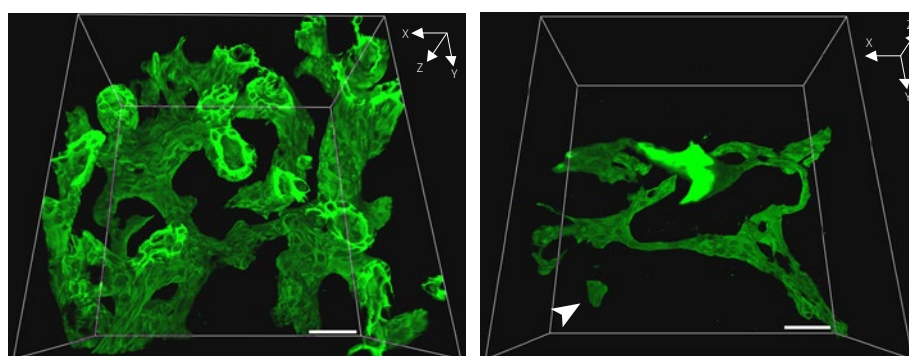
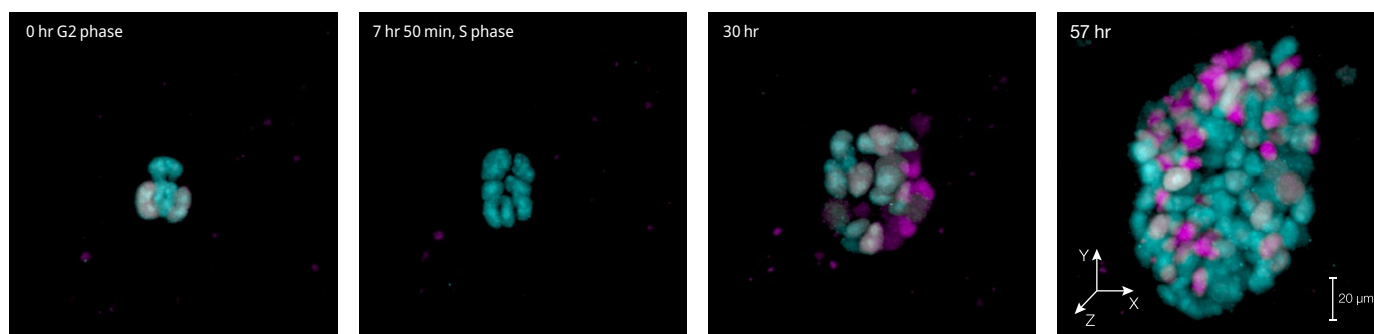


Image data courtesy of Asako Sakaue-Sawano, Atsushi Miyawaki, RIKEN Brain Science Institute Laboratory for Cell Function Dynamics  
Reference: *Development*. 2013 Nov; 140 (22): 4624–32. doi: 10.1242/dev.099226. Epub 2013 Oct 23.

## Time-Lapse Image Acquisition of Undifferentiated ES Cells (UPLSAPO30XS)

- Time-lapse observation of mouse ES cells labeled with Fucci (CA) 2.1



Undifferentiated embryonic stem (ES) cells rapidly proliferate and are very delicate. Phototoxicity during time-lapse imaging may damage ES cells and reduce their proliferation speed, making it difficult to perform time-lapse imaging of ES cells under physiologically accurate conditions. The FLUOVIEW microscope enables low-phototoxic time-lapse imaging by using extremely low laser power due to a highly efficient lightpath and sensitive detection devices. These properties enabled a research group to perform a time-lapse imaging experiment spanning 57 hours, in which three normal cell cycles of rapidly dividing undifferentiated ES cells were completely covered.

Image data courtesy of Dr. Masahiro Yo, Dr. Asako Sakaue-Sawano, and Dr. Atsushi Miyawaki (team leader), Laboratory for Cell Function Dynamics, RIKEN Center for Brain Science

# High-Resolution Objectives for Super Resolution / TIRF

A high NA is important for super resolution or total internal reflection fluorescence (TIRF) microscopy. Evident is a pioneer in TIRF microscopy, and we offer a broad lineup of objectives with numerical apertures ranging from 1.45 to the world's highest NA of 1.7\*<sup>1</sup> and magnifications ranging from 60X to 150X. In response to technology advancements such as super resolution and wide-area imaging using sCMOS cameras, we developed advanced lens manufacturing technology that enabled us to create the world's first plan corrected apochromat objective with an NA of 1.5\*<sup>2</sup>. These objectives deliver uniform image quality at a large field of view, enabling researchers to acquire high-quality raw images.

\*1 As of Oct 4, 2018. According to Evident research.

\*2 As of Oct 4, 2018. According to Evident research of objective lens using common immersion oil (refractive index  $n_e = 1.518$ ).



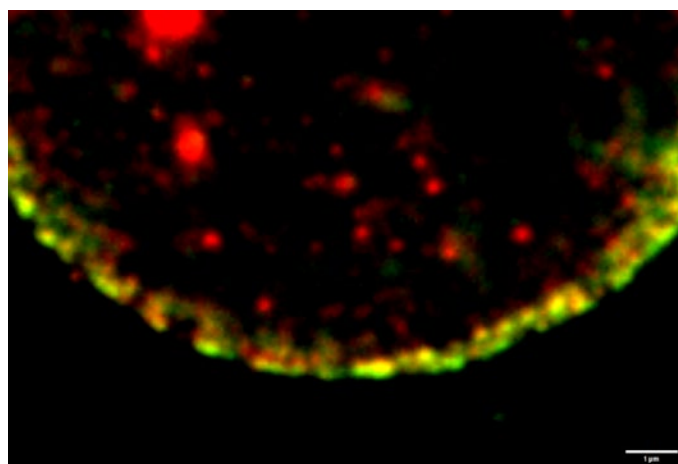
## High-Resolution Objectives for Super Resolution and TIRF

	W.D. (mm)	MAG.	OFN* <sup>3</sup>	NA	Immersion	Applications
UPLAPO60XOHR	0.11	60X	22	1.50	Oil	Whole cell TIRF imaging, real-time super resolution imaging for live cells, super resolution imaging of tiny structures, such as organelles
UPLAPO100XOHR	0.12	100X	22	1.50	Oil	Real-time super resolution imaging for live cells, super resolution imaging of tiny structures, such as organelles, high-resolution imaging of cell membranes or subcellular organelles, and single-molecule level experiments
APON100XHOTIRF	0.08	100X	22	1.70	Special Oil	Observing the movement of proteins or vesicles at the single-molecule level
UAPON150XOTIRF	0.08	150X	22	1.45	Oil	Subcellular imaging (e.g., organelle, endoplasmic reticulum, and intracellular vesicle trafficking)

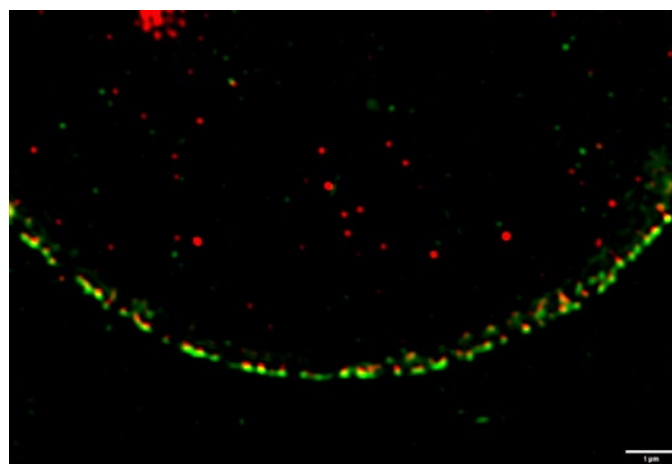
\*3 Maximum field number observable through the eyepiece.

## Real-Time Super Resolution Imaging

- Combine the UPLAPO60XOHR and UPLAPO100XOHR objectives with the SpinSR10 spinning disk confocal super resolution system.
- The SpinSR10 system quickly acquires super resolution images and offers live display with resolution down to 120 nm XY resolution.



Confocal image



Super resolution image

Green: Alexa488-labeled Nup358, which localizes to the cytoplasmic surface of the nucleopore complex.  
 Red: Alexa555-labeled Nup62, which localizes to the nucleopore complex central plug.  
 Localization of Nup358 and Nup62 can be distinguished by the super resolution technique.  
 \*Nuclear pore complex of HeLa cell.

Image courtesy of: Hidetaka Kosako, Fujii Memorial Institute of Medical Sciences, Tokushima university

## Single-Molecule Fluorescence Imaging to Count the Subunits of a Transmembrane Ion Channel Complex (APON100XHOTIRF)

- Single-molecule TIRF imaging with high-resolution, bright images and a 1.70 NA.

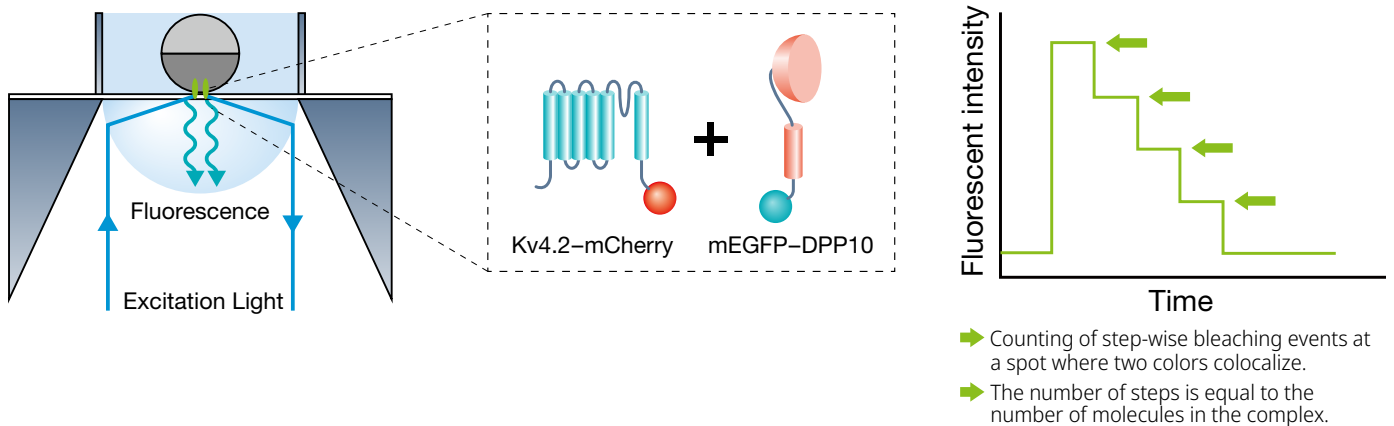
The study's subunit counting required continuous fluorescence photobleaching of proteins (subunits) that were tagged with a fluorescent protein—such as a monomeric-enhanced green fluorescent protein (mEGFP). An excitation laser was used for about 10 seconds to cause photobleaching. The process was monitored in real time using single-molecule fluorescence imaging. At the single-molecule level, fluorescence photobleaching is stepwise based on the number of fluorescent molecules. Therefore, the number of DPP10 molecules can be determined by counting the stepwise photobleaching events at the spots where Kv4.2-mCherry and mEGFP-DPP10 colocalize. The world's highest NA<sup>\*2</sup> of the APON100XHOTIRF objective enables researchers to measure fluorescence intensity change caused by single-molecule photobleaching. This study<sup>\*3</sup> revealed that a maximum of four molecules of DPP10 subunits form a complex with the ion channel Kv4.2.

\*1 Ulbrich, MH, and Isacoff EY. "Subunit counting in membrane-bound proteins." *Nature Methods*, 4 (2007): 319-321.

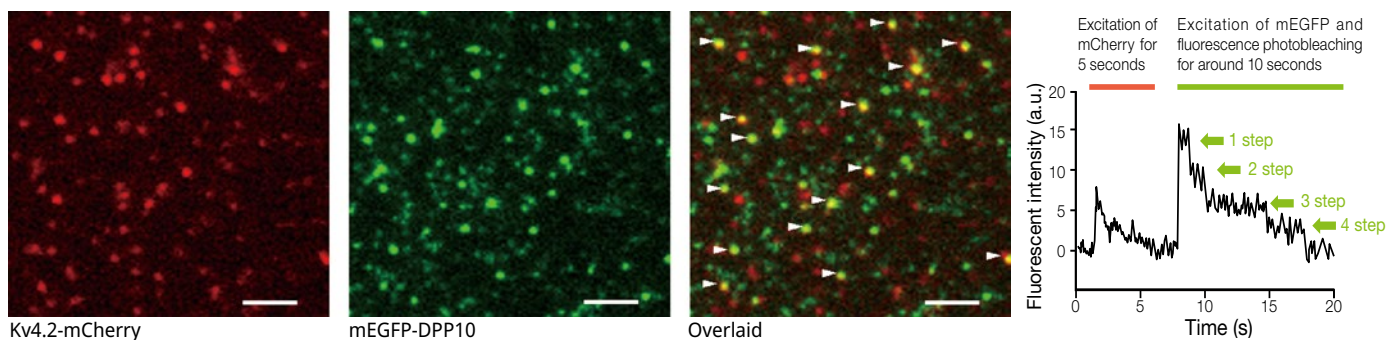
\*2 As of Oct 4, 2018. According to Evident research.

\*3 Kitazawa M, Kubo Y, and Nakajo K. "Kv4.2 and accessory dipeptidyl peptidase-like protein 10 (DPP10) subunit preferentially form a 4:2 (Kv4.2:DPP10) channel complex." *J Biol Chem*, 290 (2015): 22724-22733.

### Schematic Illustration of Subunit Counting of a Transmembrane Ion Channel Complex Using Single-Molecule Fluorescence Imaging



### Determining the Subunit Stoichiometry of the Kv4.2-DPP10 Channel Complex by Subunit Counting



Localization of Kv4.2-mCherry is visualized by excitation of mCherry in the first five seconds, followed by excitation of mEGFP in the next 10 seconds to visualize its localization and continuous fluorescence photobleaching. Spots with photobleaching of mEGFP in a maximum of 4 steps were found by graphing the change in fluorescence intensity at each spot where two colors of fluorescent molecules colocalized (indicated by the white arrow head). Therefore, it was found that a maximum of four molecules of mEGFP-DPP10 were bound in the Kv4.2 ion channel complexes. Scale bar, 20  $\mu$ m.

Image data courtesy of; Masahiro Kitazawa, Ph.D., Yoshihiro Kubo, M.D., Ph.D., Division of Biophysics and Neurobiology, Department of Molecular Physiology, National Institute for Physiological Sciences Koichi Nakajo, Ph.D., Department of Physiology, Osaka Medical College

# Super-Corrected Objective

Are your fluorescence signals really colocalized? Answering this question with standard fluorescence microscopy requires a superior optical design that corrects for color shifts (aberration) that occur when light passes through an objective. Doing this with just two or three colors is becoming increasingly insufficient. The super-corrected 60X OSC objective corrects for a broad range of color aberration to provide images that capture fluorescence in the proper location. Save time and resources in multicolor labeling experiments without having to go through post-processing adjustments.



## PLAPON60XOSC2

W.D. (mm)	0.12
MAG.	60X
OFN*	22
NA	1.40
Immersion	Oil

\*Maximum field number observable through eyepiece.

The high NA PLAPON60XOSC2 oil-immersion objective minimizes chromatic aberration in the 405–650 nm region for enhanced imaging performance and image resolution at 405 nm. The objective delivers a high degree of correction for both axial and lateral chromatic aberration to acquire 2D and 3D images with excellent reliability, accuracy, and improved colocalization analysis. The objective also compensates for chromatic aberration in the near infrared up to 850 nm.

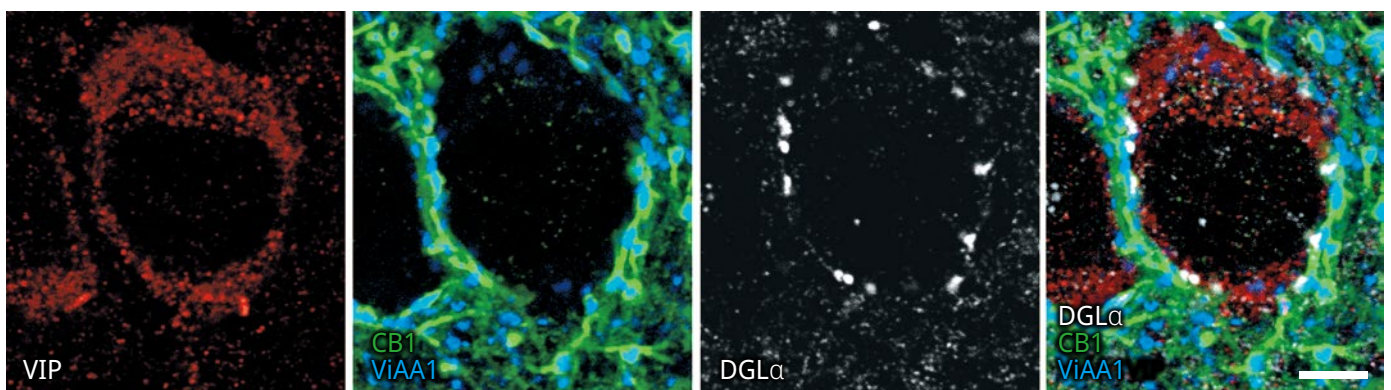
### Comparing the Performance of the PLAPON60XOSC2 and UPLXAPO60XO

	UPLXAPO60XO	PLAPON60XOSC2
On-axis vertical chromatic aberration (Z direction)	 Approx. 0.2 $\mu\text{m}$	 Approx. 0 $\mu\text{m}$
Off-axis lateral chromatic aberration (X-Y direction)	 Approx. 0.15 $\mu\text{m}$	 Approx. 0.05 $\mu\text{m}$

Comparison of chromatic aberration measured by the FLUOVIEW microscope using TetraSpeck Microsphere. cyan: 405 nm excitation, magenta: 640 nm excitation.

## Quadruple Immunofluorescence of Brain Tissue

- Improved detection sensitivity and resolution.
- Minimizes chromatic aberrations, ideal for immunofluorescence applications.



Quadruple immunofluorescence for multiple functional molecules and cell markers can provide detailed information on cell expression and subcellular localization, which includes the codependent or independent relationship between related functional cells and intercellular spatial distances. ViAA1 (Alexa Fluor405, blue), CB1 (Alexa Fluor488, green), VIP (Cy3, red), and DGL $\alpha$  (Alexa Fluor647, white). Scale bar, 5  $\mu\text{m}$ .

Image data courtesy of Masahiko Watanabe, M.D., Ph.D., Department of Anatomy, Hokkaido University Graduate School of Medicine  
Reference: *J Neurosci.* 2015 Mar 11; 35 (10): 4215–28. doi: 10.1523/JNEUROSCI.4681-14.2015.

# Save Time Imaging Plastic-Bottom Plates and Dishes

Your experiment time is valuable, and every extra step required in the process takes time away from your research goals. Inspecting tissue culture with phase contrast and fluorescence imaging and having confidence in fluorescent protein expression levels has often meant first culturing tissue in plastic-bottom dishes for adherence and then transferring the culture to glass chambers for imaging. With the UCPLFLN20XPH objective, you can skip the step of re-plating cells in glass chambers. Designed for both fluorescence and phase imaging of tissue in plastic-bottom dishes, the UCPLFLN20XPH objective helps improve your workflow. With its high NA, images are bright and even across the objective's large field of view, and the correction collar and long working distance optimizes images through different cell culture vessels.



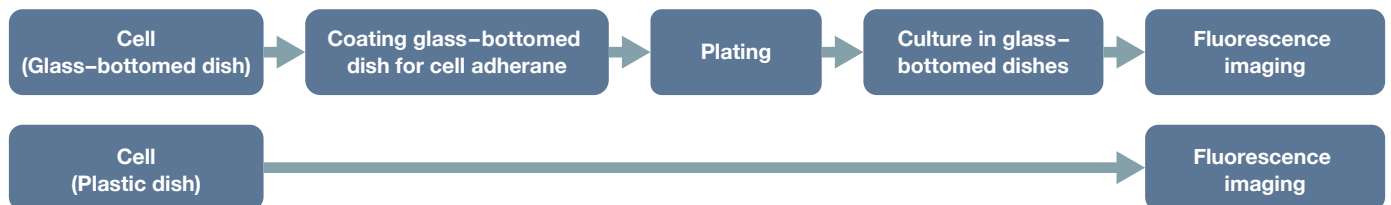
## UCPLFLN20XPH

W.D. (mm)	0.8 - 1.8
MAG.	20X
OFN*	22
NA	0.70
Immersion	Dry

\*Maximum field number observable through eyepiece.

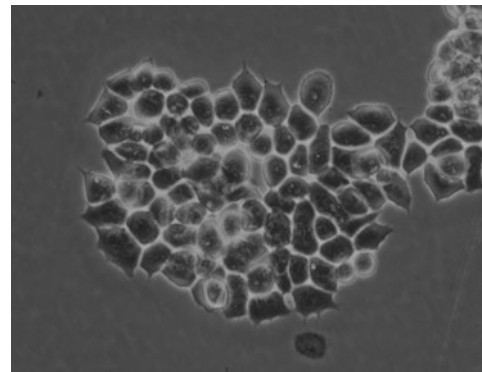
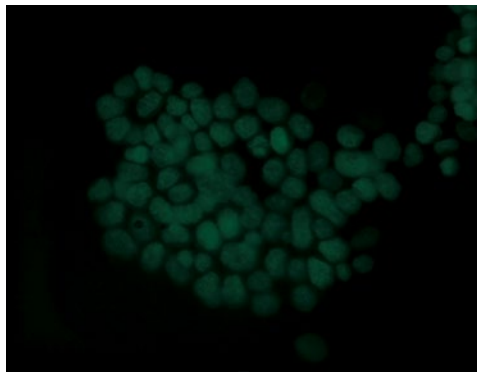
## Improve the Cell Culture Workflow

- Simplify the workflow for fluorescence observation.
- No longer necessary to subculture, which often requires an extra coating step.

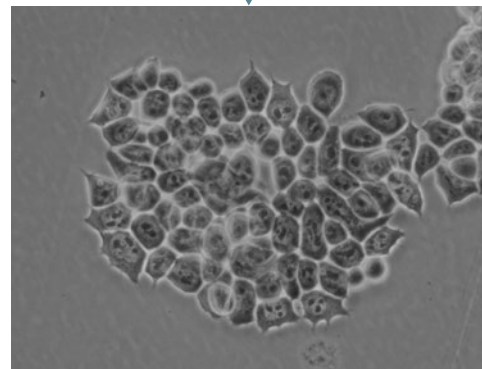
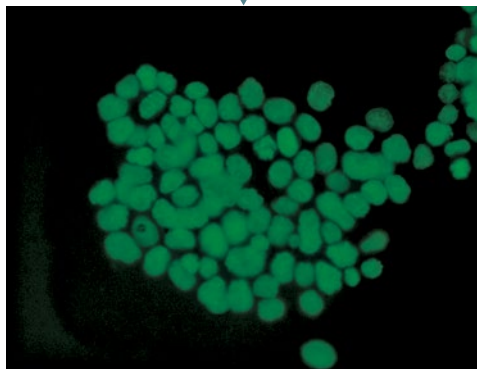


## ES cells expressing GFP-H2B in a 35 mm plastic-bottom cell culture dish

LUPLFLN20XPH  
(NA 0.45)



UCPLFLN20XPH  
(NA 0.7)



Fluorescence image

Phase contrast image

Bright fluorescence observation of histones in the nuclei (GFP-H2B) and phase contrast observation of nucleolus are possible with a high degree of detail.

Image data courtesy of: Tomonobu Watanabe, Ph.D., Laboratory for Comprehensive Bioimaging, RIKEN Quantitative Biology Center

## Immersion Oils

### Low-Autofluorescence Immersion Oil



#### IMMOIL-F30CC

- 1/10 the level of autofluorescence compared to standard oil
- Low odor – MSDS available

### Silicone Immersion Oil



#### SIL300CS-30SC

- Refractive index:  $n_e=1.406$  at 23 °C (73 °F)
- Net 30 mL
- Low autofluorescence

## List of Reference Articles Using A Line Objectives

### MPE-Dedicated Objectives

**Nat Immunol.** 2019 Feb; 20(2): 141-151. doi: 10.1038/s41590-018-0293-x. Epub 2019 Jan 14. "A noncanonical role for the engulfment gene ELMO1 in neutrophils that promotes inflammatory arthritis." Arandjelovic S, Perry JSA, Lucas CD, Penberthy KK, Kim TH, Zhou M, Rosen DA, Chuang TY, Bettina AM, Shankman LS, Cohen AH, Gaultier A, Conrads TP, Kim M, Elliott MR, Ravichandran KS.

**Nature.** 2019 Jan; 565(7739): 366-371. doi: 10.1038/s41586-018-0812-9. Epub 2018 Dec 31. "Tissue-resident memory CD8+ T cells promote melanoma-immune equilibrium in skin." Park SL, Buzzai A, Rautela J, Hor JL, Hochheiser K, Effern M, McBain N, Wagner T, Edwards J, McConville R, Wilmott JS, Scolyer RA, Tüting T, Palendria U, Gyorki D, Mueller SN, Huntington ND, Bedoui S, Hölzel M, Mackay LK, Waithman J, Gebhardt T.

**Immunity.** 2018 Oct 16; 49(4): 654-665.e5. doi: 10.1016/j.immuni.2018.07.014. Epub 2018 Sep 25. "A Metabolism-Based Quorum Sensing Mechanism Contributes to Termination of Inflammatory Responses." Postaj J, Olekhnovitch R, Lemaître F, Bousso P.

**Neuron.** 2018 Oct 10; 100(1): 244-258.e12. doi: 10.1016/j.neuron.2018.08.016. Epub 2018 Aug 30. "Thalamocortical Axonal Activity in Motor Cortex Exhibits Layer-Specific Dynamics during Motor Learning." Tanaka YH, Tanaka YR, Kondo M, Terada SI, Kawaguchi Y, Matsuzaki M.

**Cell Metab.** 2018 Jul 3; 28(1): 69-86.e6. doi: 10.1016/j.cmet.2018.06.006. "Targeting Breast Cancer Stem Cell State Equilibrium through Modulation of Redox Signaling." Luo M, Shang L, Brooks MD, Jiaoge E, Zhu Y, Buschhaus JM, Conley S, Fath MA, Davis A, Gheordunescu E, Wang Y, Harouaka R, Lozier A, Triner D, McDermott S, Merajver SD, Luker GD, Spitz DR, Wicha MS.

**Cancer Cell.** 2018 May 14; 33(5): 937-948.e8. doi: 10.1016/j.ccell.2018.03.021. Epub 2018 Apr 19. "Germline Genetic IKZF1 Variation and Predisposition to Childhood Acute Lymphoblastic Leukemia." Churchman ML, Qian M, Te Kronnie G, Zhang R, Yang W, Zhang H, Lana T, Tedrick P, Baskin R, Verbit K, Peters JL, Devidas M, Larsen E, Moore JM, Gu Z, Qu C, Yoshihara H, Porter SN, Pruett-Miller SM, Wu G, Raetz E, Martin PL, Bowman WP, Winick N, Mardis E, Fulton R, Stanulla M, Evans WE, Relling MV, Pui CH, Hunger SP, Loh ML, Handgretinger R, Nichols KE, Yang JJ, Mullighan CG.

**Biochem Biophys Res Commun.** 2018 Jun 2; 500(2): 236-241. doi: 10.1016/j.bbrc.2018.04.049. Epub 2018 Apr 18.

"A spherical aberration-free microscopy system for live brain imaging." Ue Y, Monai H, Higuchi K, Nishiwaki D, Tajima T, Okazaki K, Hama H, Hirase H, Miyawaki A.

**Nat Neurosci.** 2018 Apr; 21(4): 625-637. doi: 10.1038/s41593-018-0109-1. Epub 2018 Mar 5. "A three-dimensional single-cell-resolution whole-brain atlas using CUBIC-X expansion microscopy and tissue clearing." Murakami TC, Mano T, Saikawa S, Horiguchi SA, Shigeta D, Baba K, Sekiya H, Shimizu Y, Tanaka KF, Kiyonari H, Iino M, Mochizuki H, Tainaka K, Ueda HR.

**Science.** 2018 Mar 30; 359(6383): 1524-1527. doi: 10.1126/science.aao0702. Epub 2018 Feb 8. "Hippocampal ripples down-regulate synapses." Norimoto H, Makino K, Gao M, Shikano Y, Okamoto K, Ishikawa T, Sasaki T, Hioki H, Fujisawa S, Ikegaya Y.

### Silicone Immersion Objectives

**PLoS Biol.** 2018 Sep 26; 16(9): e2004874. doi: 10.1371/journal.pbio.2004874. eCollection 2018 Sep. "mDia1/3 generate cortical F-actin meshwork in Sertoli cells that is continuous with contractile F-actin bundles and indispensable for spermatogenesis and male fertility." Sakamoto S, Thumkeo D, Ohta H, Zhang Z, Huang S, Kanchanawong P, Fuu T, Watanabe S, Shimada K, Fujihara Y, Yoshida S, Ikawa M, Watanabe N, Saitou M, Narumiya S.

**Cell.** 2018 Jul 12; 174(2): 481-496.e19. doi: 10.1016/j.cell.2018.06.042. "A Genetically Encoded Fluorescent Sensor Enables Rapid and Specific Detection of Dopamine in Flies, Fish, and Mice." Sun F, Zeng J, Jing M, Zhou J, Feng J, Owen SF, Luo Y, Li F, Wang H, Yamaguchi T, Yong Z, Gao Y, Peng W, Wang L, Zhang S, Du J, Lin D, Xu M, Kreitzer AC, Cui G, Li Y.

**J Neurosci.** 2018 May 2; 38(18): 4329-4347. doi: 10.1523/JNEUROSCI.3644-17.2018. Epub 2018 Apr 24. "GABAergic Local Interneurons Shape Female Fruit Fly Response to Mating Songs." Yamada D, Ishimoto H, Li X, Kohashi T, Ishikawa Y, Kamikouchi A.

**Dev Cell.** 2018 Mar 12; 44(5): 611-623.e7. doi: 10.1016/j.devcel.2018.01.020. Epub 2018 Feb 22. "Activation of the Notch Signaling Pathway In Vivo Elicits Changes in CSL Nuclear Dynamics." Gomez-Lamarca MJ, Faló-Sanjuán J, Stojnic R, Abdul Rehman S, Muresan L, Jones ML, Pillidge Z, Cerda-Moya G, Yuan Z, Baloul S, Valenti P, Bystrycky K, Payre F, O'Holleran K, Kovall R, Bray S.J.

**Development.** 2018 Mar 1; 145(5): pii: dev154617. doi: 10.1242/dev.154617. "An evolutionarily conserved NIMA-related kinase directs rhizoid tip growth in the basal land plant *Marchantia polymorpha*." Otani K, Ishizaki K, Nishihama R, Takatani S, Kohchi T, Takahashi T, Motose H.

### High-Resolution Objectives for Super Resolution and TIRF

**Cell.** 2018 Nov 15; 175(5): 1430-1442.e17. doi: 10.1016/j.cell.2018.09.057. Epub 2018 Oct 25. "Visualizing Intracellular Organelle and Cytoskeletal Interactions at Nanoscale Resolution on Millisecond Timescales." Guo Y, Li D, Zhang S, Yang Y, Liu JJ, Wang X, Liu C, Milkic DE, Moore RP, Tulu US, Kiehart DP, Hu J, Lippincott-Schwartz J, Betzig E, Li D.

**Proc Natl Acad Sci U S A.** 2018 Oct 9; 115(41): 10363-10368. doi: 10.1073/pnas.1806727115. Epub 2018 Sep 25. "The Atg2-Atg18 complex tethers pre-autophagosomal membranes to the endoplasmic reticulum for autophagosome formation." Kotani T, Kirisako H, Koizumi M, Ohsumi Y, Nakatogawa H.

**Nat Cell Biol.** 2018 Oct; 20(10): 1118-1125. doi: 10.1038/s41556-018-0192-2. Epub 2018 Sep 17. "Single particle trajectories reveal active endoplasmic reticulum luminal flow." Holcman D, Parutto P, Chambers JE, Fantham M, Young LJ, Marciniak SJ, Kaminski CF, Ron D, Avezov E.

**Nature.** 2018 Sep; 561(7721): 63-69. doi: 10.1038/s41586-018-0466-7. Epub 2018 Aug 29. "Role of glutamine synthetase in angiogenesis beyond glutamine synthesis." Eelen G, Dubois C, Cantelmo AR, Goveia J, Brünig U, DeRan M, Jarugumilli G, van Rijsel J, Saladino G, Comitani F, Zecchin A, Rocha S, Chen R, Huang H, Vandekerke S, Kalucka J, Lange C, Morales-Rodriguez F, Cruys B, Treps L, Ramer L, Vinckier S, Brepoels K, Wyns S, Souffreau J, Schoonjans L, Lamers WH, Wu Y, Haestraete J, Hofkens J, Liekens S, Cubbon R, Ghesquière B, Dewerchin M, Gervasio FL, Li X, van Buul JD, Wu X8, Carmeliet P.

**Nat Methods.** 2018 Jun; 15(6): 425-428. doi: 10.1038/s41592-018-0004-4. Epub 2018 May 7. "Single-shot super-resolution total internal reflection fluorescence microscopy." Guo M, Chandris P, Giannini J, Trexler AJ, Fischer R, Chen J, Vishwasrao HD, Rey-Suarez I, Wu Y, Wu X, Waterman CM, Patterson GH, Upadhyaya A, Taraska JW, Shroff H.

**Cell Host Microbe.** 2018 Jun 13; 23(6): 786-795.e5. doi: 10.1016/j.chom.2018.05.006. "The Listeriolysin O PEST-like Sequence Co-opts AP-2-Mediated Endocytosis to Prevent Plasma Membrane Damage during Listeria Infection." Chen C, Nguyen BN, Mitchell G, Margolis SR, Ma D, Portnoy DA.

**Nat Biotechnol.** 2018 Jun; 36(5): 451-459. doi: 10.1038/nbt.4115. Epub 2018 Apr 11. "Fast, long-term, super-resolution imaging with Hessian structured illumination microscopy." Huang X, Fan J, Li L, Liu H, Wu R, Wu Y, Wei L, Mao H, Lal A, Xi P, Tang L, Zhang Y, Liu Y, Tan S, Chen L.

**Nat Chem Biol.** 2018 May; 14(5): 497-506. doi: 10.1038/s41589-018-0032-5. Epub 2018 Apr 2. "Super-long single-molecule tracking reveals dynamic-anchorage-induced integrin function." Tsunoyama TA, Watanabe Y, Goto J, Naito K, Kasai RS, Suzuki KGN, Fujiwara TK, Kusumi A.

### Super-Corrected 60X Objective

**Mol Cell.** 2018 Jul 5; 71(1): 25-41.e6. doi: 10.1016/j.molcel.2018.05.018. Epub 2018 Jun 21. "Histone Methylation by SETD1A Protects Nascent DNA through the Nucleosome Chaperone Activity of FANCD2." Higgs MR, Sato K, Reynolds JJ, Begum S, Bayley R, Goula A, Vernet A, Paquin KL, Skalkin DG, Kobayashi W, Takata M, Howlett NG, Kurumizaka H, Kimura H, Stewart GS.

**Nat Commun.** 2018 Apr 11; 9(1): 1400. doi: 10.1038/s41467-018-03845-1. "Histone H3.3 sub-variant H3mm7 is required for normal skeletal muscle regeneration." Harada A, Maehara K, Ono Y, Taguchi H, Yoshioka K, Kitajima Y, Xie Y, Sato Y, Iwasaki T, Nogami J, Okada S, Komatsu T, Semba Y, Takemoto T, Kimura H, Kurumizaka H, Ohkawa Y.

To select the right objective for your application, please use our Objective Finder tool:

[olympus-lifescience.com/objective-finder](https://olympus-lifescience.com/objective-finder)

#### • EVIDENT CORPORATION is ISO14001 certified.

For details on certification registration, visit <https://www.olympus-lifescience.com/en/support/iso/>

#### • EVIDENT CORPORATION is ISO9001 certified.

\* All company and product names are registered trademarks and/or trademarks of their respective owners.  
\* Specifications and appearances are subject to change without any notice or obligation on the part of the manufacturer.  
\* Illumination devices for microscope have suggested lifetimes. Periodic inspections are required. Please visit our website for details.

[EvidentScientific.com](https://www.evidentscientific.com)

**EVIDENT**

EVIDENT CORPORATION

Shinjuku Monolith, 2-3-1 Nishi-Shinjuku, Shinjuku-ku, Tokyo 163-0910, Japan

**OLYMPUS**

N8600506-102023